A Biologically Inspired Multimodal Whisker Follicle

Hasitha Wegiriya, Nantachai Sornkarn, Harry Bedford and Thrishantha Nanayakkara
Centre for Robotics Research, Department of Informatics,
Kings College London, Strand WC2R 2LS, London, UK.
E-mail: {hasitha.wegiriya, nantachai.sornkarn, harry.bedford, thrish.antha}@kcl.ac.uk

***Abstract*—Mammalian whisker follicle contains multiple sensory receptors strategically organized to capture tactile sensory stimuli of different frequencies via the vibrissal system. There have been a number of attempts to develop robotic whiskers to perform texture classification tasks in the recent past. Inspired by the features of biological whisker follicle, in this paper we design and use a novel soft whisker follicle comprising of two different frequency-dependent data capturing modules to derive deeper insights into the biological basis of tactile perception in the mammalian whisker follicle. In our design, the innervations at the Outer Conical Body (OCB) of a biological follicle are realized by a piezoelectric transducer for capturing high frequency components; whereas the innervations around the hair Papilla are represented by a hall sensor to capture low frequency components during the interaction with the environment. In this paper, we show how low dimensional information such as the principle components of co-variation of these two sensory modalities vary for different speeds and indentations of brushing the whisker against a surface. These new insights into the biological basis of tactile perception using whiskers provides new design guidelines to develop efficient robotic whiskers.**

***Index Terms*—Robotic Whiskers, A Biologically Inspired Multimodal Whisker Follicle, Tactile Sensor**

I. INTRODUCTION

Tactile sensing is one of the most important and complex sensory systems for most living beings. In order to acquire tactile information and explore the environment, animals use a wide range of biological mechanisms and transduction techniques. Whiskers, or *vibrissae* are a form of mammalian hair, found on almost all mammals other than Homo Sapiens. For many mammals, and especially rodents, these whiskers are essential as a means of tactile sensing. Whiskers differ from regular pelage hair in the several ways, as detailed by A.S Ahl [1].

Most research on whiskers has been done on the mystacial pad on rodents. The mystacial pad concerns the area directly under the nose, and comprises a highly uniform array of whiskers of varying length [2]. Whilst not all whiskers move, the mystacial pad of rodents is musculated, allowing the mammal hosts to 'whisker' - a motion of swaying the whiskers back and forth [3]. In rats, whisking happens at a dominant frequency of 8Hz [4]. Whilst intrinsic and extrinsic muscles allow 'whisking' to occur, the whole mystacial pad is also changeable in shape [3]. As a tactile sensor array, this means the mystacial pad is highly adaptable with several degrees of freedom.

In terms of anatomy, the whisker itself is not sensitive. Instead, all the transduction occurs at the follicle. Each follicle has precisely one whisker, a rich blood supply, and one or more sebaceous glands [1]. Again, unlike other hair follicles that use arrector pili, (involuntary muscles), the muscles attached to whiskers are striated, or voluntarily controlled. Moreover, each follicle is connected to a blood filled sinus, which each have a selection of different nerve receptors. These nerve receptors include Pacinilike corpuscles, Merkel receptors, straight lanceolate terminals, branched circular lanceolate receptors, branched lanceolate endings, and endings of unmyelinated nerve fibers [1]. A single whisker sensor system may contain hundreds of these mechanoreceptors [5]. Indeed, the mechanoreceptors are known to encode information about small deflections, velocity, direction and amplitude of deflections [5].

Whiskers have therefore been the focus of several works concerning artificial tactile sensors. Older whisker sensor designs, such as that of Russell [6][7], employ rigid whiskers as levers, with a means of measuring an angle change. Russell used a potentiometer - a resistive transducer - to determine the angle of deflection in his 2002 work. Most designs use simple transduction techniques - the focus is instead on the mechanical properties of the whisker, and array organization.

As Russell notes, it is not always necessary to overcomplicate the design with 'extra circuitry and wiring', if a series of simple devices is capable of achieving the same outcome [7]. For instance, a simple whisker attached to capacitor microphones has been able to discriminate between four different textures [8] with approximately a 70% success rate after only one sweep. Similar simple designs include that of Solomon and Hartmann, who used (piezoresistive) strain gauges to measure the deviation of four steel whiskers in two dimensions [9]. They used a novel technique that comprised of measuring the bending moment at the base of a whisker, in order to determine the point of contact along its length. By rotating the array around the object, they were able to correctly map the object in three dimensions [9][10]. Kim and Moller used the same technique, with hall sensors instead of strain gauges [11].

Whilst these works illustrate that simple sensor designs can achieve good results, the designs themselves are much more focused on the direct sensing of objects and their properties, instead of *'the control of whiskers [whisking] and the impact of this control on sensing'*, as Pearson et al. state [10]. They focus their work on developing a whisking pattern with the aim of *'minimal impingement/maximal contact (MIMC)'* [10], meaning whiskers touch objects as often as possible, but with least force as possible.

The more recent 'ShrewBot' uses individually actuated

978-1-5090-1897-0/16/$31.00

whiskers, like in nature. These are based on the renowned 'Biotact' sensor [12]. The Biotact sensor is inspired from biology in several aspects such as the vibrissal morphology, actuation and control of whiskers, and the vibrissal sensory processing. The sensory part of the Biotact sensor is, like Kim and Moller's work, a Hall Effect device, with a small permanent magnet [12]. Sullivan et al. concluded that '*the performance of both these approaches to classify textures after training on as few as one or two surface contacts was improved when the whisking motion was controlled using a sensory feedback mechanism*'. This shows, as Pearson et al. agree, that whilst the fundamental sensor has not changed, a distinct sensory advantage can be obtained when vibrissae are actuated intelligently.

The several examples discussed here all employ previously-existing technologies (sensors) in order to transduce the sensory information. In most literature, the focus is upon sensing modalities and not on the design of the whisker itself. There is therefore scope to investigate aspects such as optimal curvature, length and the material of whiskers. Furthermore, as Pearson et al. state, the motion of whisking is another important feature that should be considered in whisker-based sensors. This paper details a whisker sensor that relies on whisking motions in order to identify different textures, through the application of multiple sensors.

II. Methodology

A. Whisker Sensor

The whisker sensor shown in figure 1 comprises a carbon fiber shaft embedded into a 3D printed cylindrical cantilever. The carbon-fiber shaft and 3-D printed cylindrical cantilever are connected via a soft silicon rubber (Ecoflex 00-10) joint. The carbon fiber shaft, of diameter 0.5mm and total length 200mm, passes through the piezoelectric sensor. This is attached to a magnet holder, containing a magnet of diameter 2 mm. The Hall effect sensor is mounted at the base of 3-D printed cylinder and linear to carbon fiber shaft (Whisker shaft). The whisker shaft is directly connected to the center of the piezoelectric sensor and placed on the magnet holder at a distance of 4 mm from the cylindrical body. Both sensors are connected to an analog to digital (AD) converter to measure their voltages.

B. Characterization of the Sensor

The sensitivity of the sensors depends on the vibration of the whisker shaft. When external vibrations are applied to the whisker shaft, the shaft deforms, and in turn, induces similar vibrations on the piezoelectric sensor. This displaces the magnet inside, causing a change in magnetic flux near the hall effect sensor. This effect generates high-frequency electrical signals from the piezoelectric sensor and low frequency signals from the hall effect sensor.

C. Experimental Setup

The experimental setup is shown in figure 2. The whisker sensor is horizontally attached to a rigid L-shape arm made

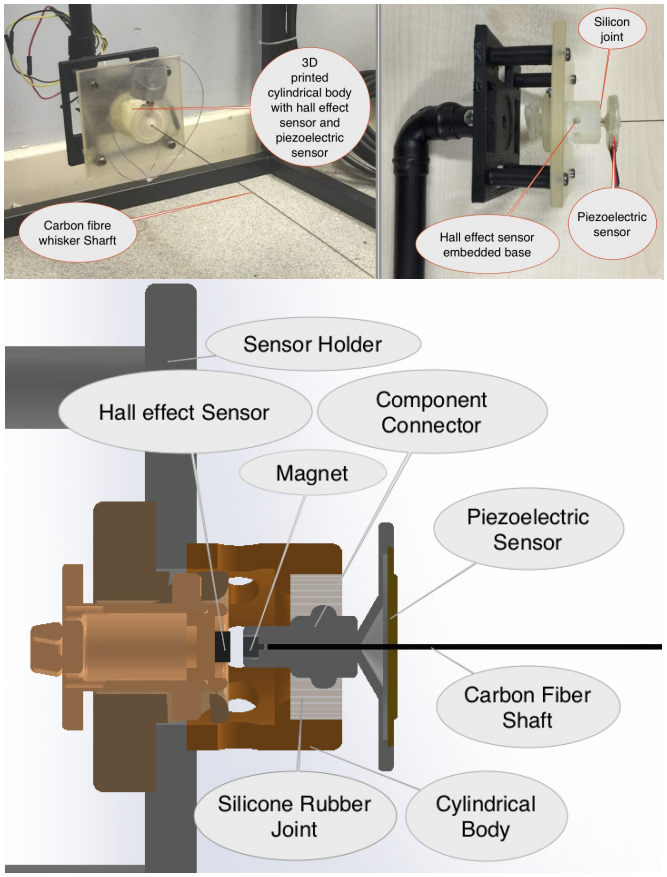

Fig. 1. Constructed Whisker Sensor. The hall sensor is mounted inside the cylindrical body. The back end of the carbon fiber shaft is attached to a component connector which holds the permanent magnet. The distance between the hall sensor and the permanent magnet was optimized based on the flux induced by the magnet.

with copper pipe and 3D printed ABS plastic. The longer side of the arm is vertically mounted to the liner stage of an XY table (Aerotech- ANT130-160-XY-25DU-XY-CMS LOWER) to allow the whisker sensor to move in x and y directions. This linear stage is capable of moving up to 50mm/s. The whisker sensor signals are sent to a National Instrument NI USB-6341 analog to digital converter. The corresponding sampling rate of the AD converter is 1000Hz. In order to control the AD converter and XY linear stages, the set-up is connected to a computer with LabView2012, a National Instruments Corp. software. The software synchronizes data retrieval and the liner stage motion. Data is then processed using MatLab R2013b, Mathworks Inc. software, which runs on an Intel Core i5 2.3GHz (64 bit) computer with 4 GB (RAM) of internal memory.

D. Experiment Process

In the experiment, the whisker is programmed to probe along the riddle side of a textured object sample. Here, we use a plastic pipe with uniform and constant riddle throughout the surface (see Figure 2(ii)). The plastic pipe sample is fixed to the external holder and placed perpendicular to the whisker

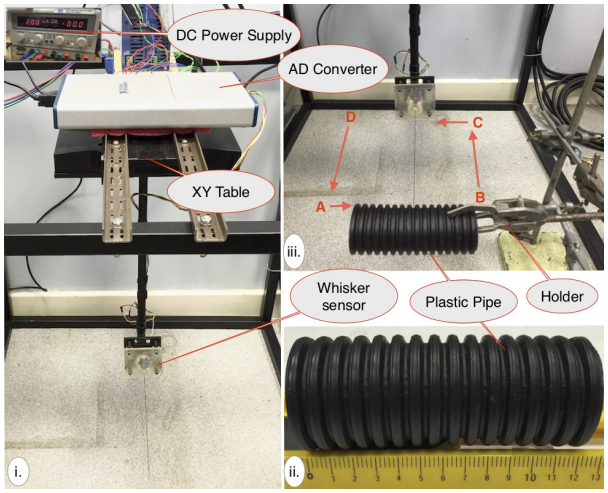

Fig. 2. Experimental Setup, (i.) Hardware Setup, (ii.) Plastic Pipe, (iii.) Programmed Path - ABCD (Data recording starts when the Whisker shaft moving from A position to B, then data recording stops and sensor goes on the B,C,D route. When the sensor moving from D to A, program select the contact indentation and selected indentation added to D to A distance, then proceed on the square path.)

shaft (figure 2(iii)). The whisker sensor comes into contact with the surface of the material, by following the path shown in figure 2(iii). The contact indentation of the whisker shaft is controlled through a component parallel to the x-axis, and contact velocity through a component along the y-axis. Both of these movements are controlled through usage of the XY table. In this experiment, we use 0 mm, 1mm, 2 mm, 3 mm, 4 mm, 5 mm indentation levels and 20 mm/sec, 15 mm/sec, 10 mm/sec, 5 mm/sec, 2 mm/sec contact speeds. Initially the indentation is set to 0mm, which provides a 'smooth touch' between the whisker and surface of the material. The corresponding contact speed of the whisker sensor is set to 20 mm/s. In a set of trials, the whisker successfully moved the programmed stroke length, and returned to its initial position via the programmed path. For each combination of indentations and contact speeds, we collected data for 20 trials. Each trial contains 120 data samples. Therefore, for a given speed of contact, the five indentation levels gave 600 samples.

III. Results

Figure 3 shows hall sensor data for speeds, $v = 2$ and 20 mm/sec and indentation levels, $\delta = 1$ and 5 mm out of $v = 2, 5, 10, 15$, and 20 mm/sec, and indentations $\delta = 0, 1, 2, 3, 4$, and 5 mm. It can be observed that the increase in δ causes an increase in the magnitude of readings in the hall sensor (Figure 3 (B) and (D)). Since the magnitude of hall sensor readings depends on the magnitude of relative movements between the hall sensor and the permanent magnet, this indicates that higher indentation level causes higher amplitudes of vibrations at the bottom end of the whisker.

Figure 4 shows piezoelectric sensor data for speeds, $v = 2$ and 20 mm/sec and indentation levels, $\delta = 1$ and 5 mm. Unlike the hall sensor, we can notice that higher indentations

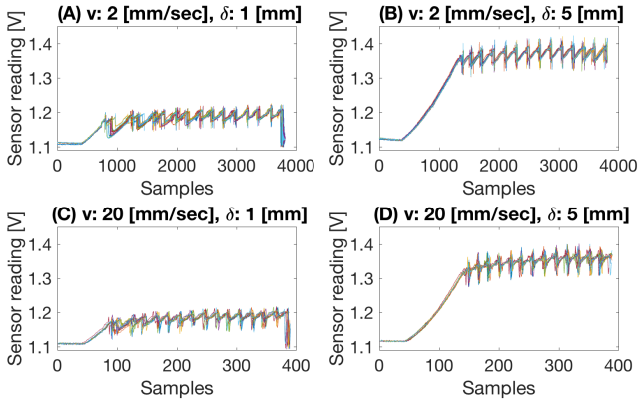

Fig. 3. Hall sensor readings for two speeds and two indentation levels of brushing the whisker against the object shown in figure 2. The experiments were conducted for 5 speeds and 6 indentation levels. The plots show data from 20 trials for each speed-indentation combination.

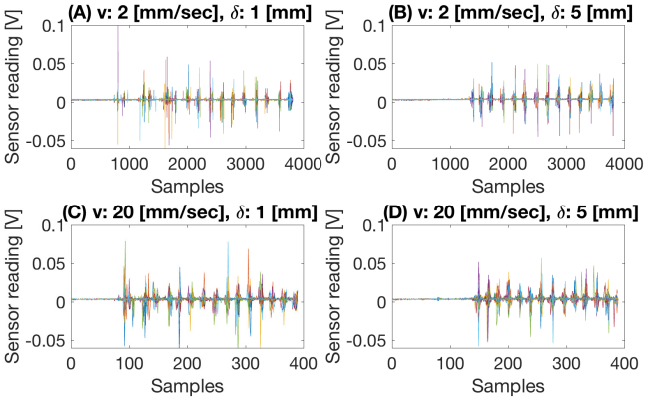

Fig. 4. Piezoelectric sensor readings for two speeds and two indentation levels of brushing the whisker against the object shown in figure 2. The plots show data from 20 trials for each speed-indentation combination.

cause relatively lower peak amplitudes in piezoelectric sensor readings (Figure 4 (B) and (D)). Apparently, this figure also shows that higher speeds give higher frequencies of vibrations (Figure 4 (C) and (D)). Since piezoelectric transducers give readings proportional to the stress exerted on them, this implies that higher indentations cause lower stresses on the pivot point at which the piezoelectric transducer is mounted.

Next we looked at the co-variance of the readings of these two sensors across different speeds and indentation levels for multiple trials. Figure 5 illustrates the scatter plot for co-variation of readings given different speeds of brushing on the object shown in figure 2. We notice that the spread of the distributions increase with increasing speed of brushing though the average values do not change significantly. This raises to question as to whether the direction of the principle components (eigen vectors of the co-variance matrix) gives higher variability when the speed of brushing increases.

Figure 7 shows the scatter plot for co-variation of readings given different indentations of brushing on the object shown

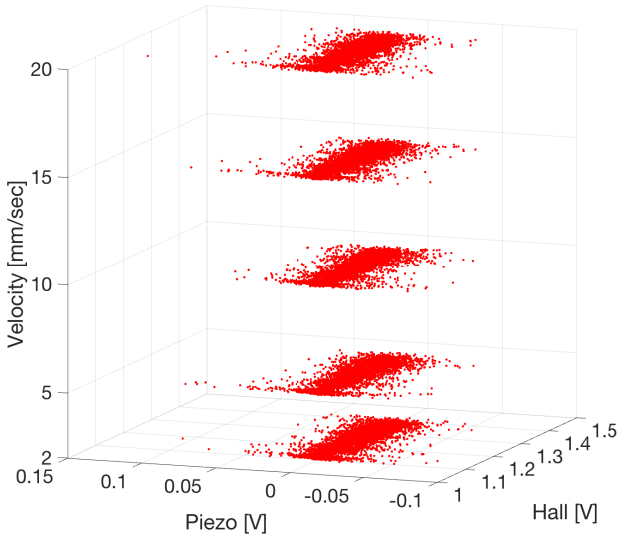

Fig. 5. The co-variation of hall sensor and piezosensor data across 5 speeds for all 6 indentation levels.

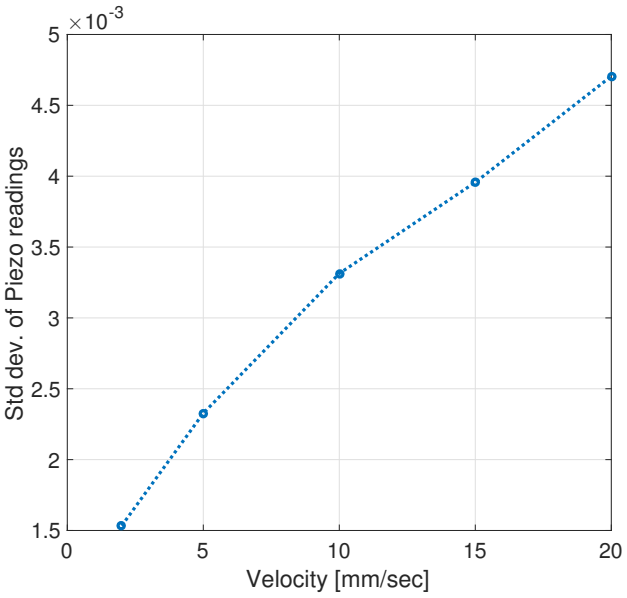

Fig. 6. The stranded deviation of piezosensor data across 5 speeds for all 6 indentation levels.

in figure 2. We notice that the major axis of the distribution rotates toward the hall sensor axis with higher indentations. This implies that the most significant principle component (the eigen vector of the co-variance matrix with largest eigenvalue) rotates from the piezosensor axis to the hall sensor axis when the indentation increases.

As observed in figure 5, 6 and 7, the changes in the behavioral variables of the whisker could lead to the change in the geometrical properties of the correlation of the sensors' responses. These provide valuable insights into possible methods for information gain about an object by varying the speed

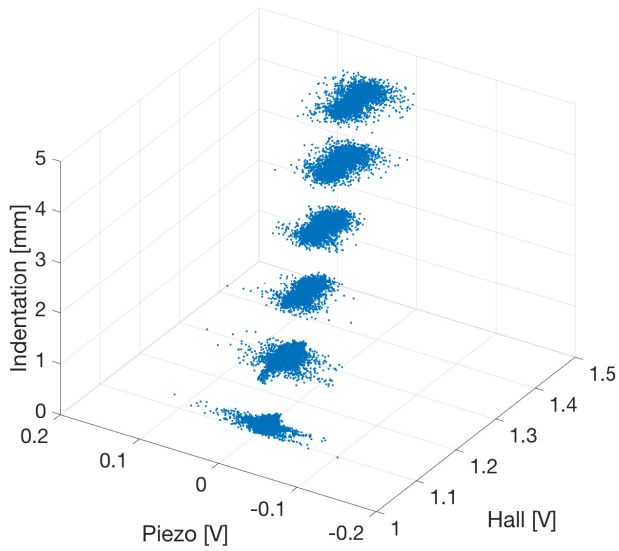

Fig. 7. The co-variation of hall sensor and piezosensor data across 6 indentation levels for all 5 speed levels.

and indentation of brushing the whisker with a follicle design proposed in this paper.

As a result of probing behavioral changes (speed and indentation), we further analyzed the relationship between the co-variation of sensor readings. The eigenvectors and eigenvalues of the co-variance matrix, for the hall and piezoelectric sensors, were obtained for each reading. Figure 8 shows the behavior of the maximum eigenvalue and the angle of the corresponding eigenvector across indentation levels for all speeds of brushing. We notice that the maximum eigenvalue increases and settles down at a stable value when the indentation increases as shown in Figure 8(A). The angle of the eigenvector with the highest eigenvalue too settles down in a stable region as shown in figure 8(B). Figure 8(C) shows that the standard deviation of the variability of the maximum eigenvalue increases and then decreases with the increasing indentation. Figure 8(D) shows that standard deviation of the angle of the eigenvector corresponding to the maximum eigen value converges to a stable region with increasing indentation levels.

If the conditional probability distribution of the maximum eigenvalue is given by $p(\lambda|\delta, v)$, where λ is the value of the maximum eigen value, the transfer entropy is given by

$$G = \sum_{\forall v \in \Re} p(\lambda|\delta, v) \log |\frac{p(\lambda|\delta, v)}{p(\lambda|\delta_0, v)}| \quad (1)$$

where δ_0 is the initial indentation, v is the speed of brushing the whisker on the object, and δ is the indentation. According to equation 1, a decrease in the width of $p(\lambda|\delta, v)$ would result in a drop and settling down of the the transfer entropy, G (a measure of the information gained by varying the indentation across all speeds), as shown in Figure 9. This implies that

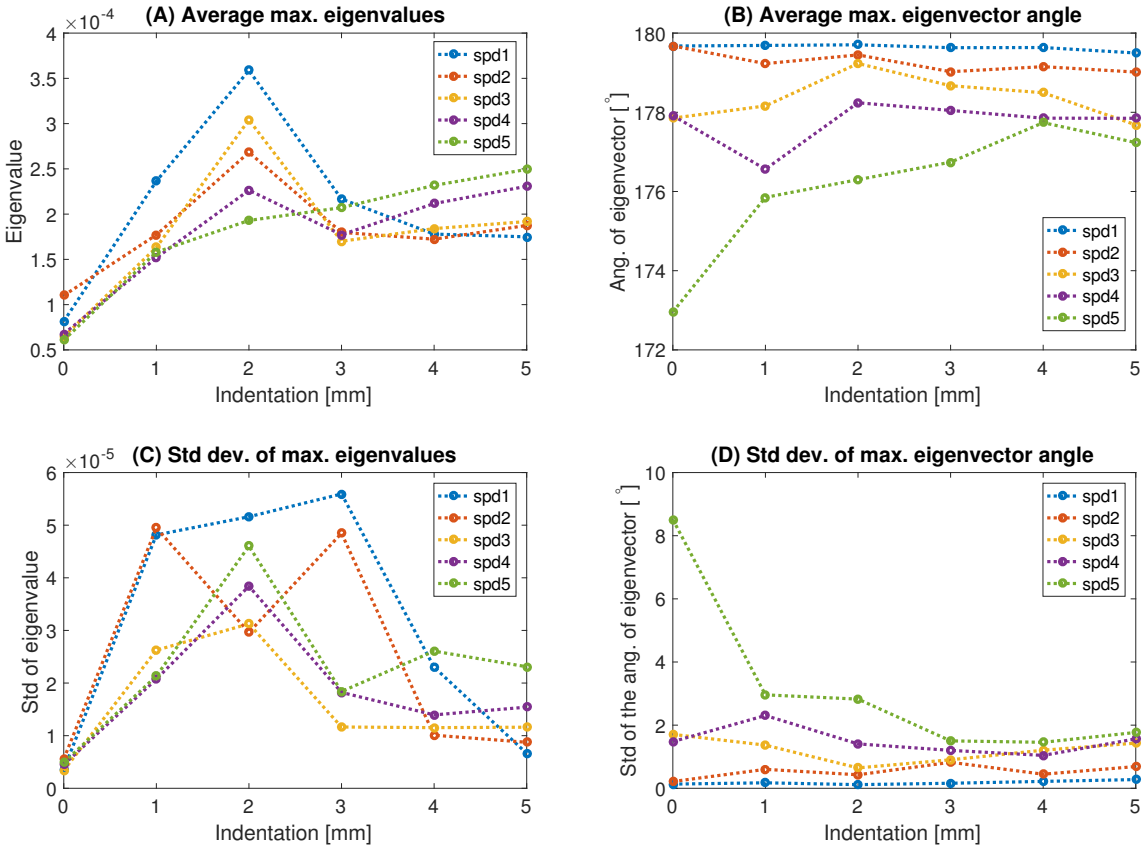

Fig. 8. Average behavior of maximum eigenvalues of the covariance matrix for hall sensor and piezosensor readings across different indentation levels and speeds of brushing the whisker.

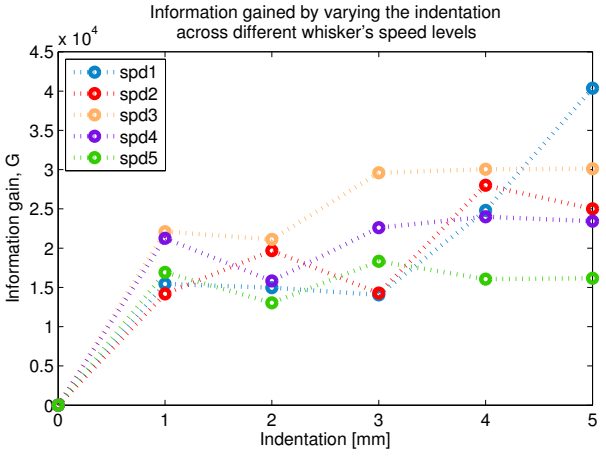

Fig. 9. The transfer entropy measured by the information gained during the variation of indentation levels across different whisker's speed levels

indentations higher than a certain range is not going to yield more information.

Figure 8 also shows that higher speeds of brushing the whisker shows highest sensitivity to changes in indentation. For instance, in figures Figure 8(B) and (C), the curve corresponding to speed-4 shows highest rate of change.

IV. Discussion and Conclusion

This paper details a novel whisker sensor system, that incorporates two different sensors, used in order to transduce information regarding textures of a sample object. The hall-effect sensor and piezoelectric sensor provide frequency-dependent data relative to vibrations on a carbon-fiber whisker shaft. The whole system is movable, and is therefore capable of producing 'whisking' movements. The design was tested for different levels of contact speed and indentation.

The maximum eigenvalue of the covariance matrix for the two sensors in the follicle - piezoelectric and hall sensor - represents the overall sensitivity of the whisker system. The angle of the eigenvector corresponding to the maximum eigenvalue gives the relative contribution made by the two sensors in the follicle. From analysis of the results in the previous section, we can conclude that increasing indentation causes the maximum eigenvalue to increase, before it settles at a stable value. The angle of the eigenvector corresponding to the highest eigenvalue and its variability is sensitive to

the speed of whisking at lower indentation levels. They settle down at a steady range beyond an indentation of 3mm.

These results indicate that the information gain of low and high frequency features of the object can be controlled by selectively controlling the whisking speed and indentation within an optimum range. This not only provides new insights to design multimodal robotic whisker follicles, but also sheds light on our understanding about the functionality of mammalian whisker follicles.

The experimental result presented in this paper agree with previous claims and methods shown in previous studies. For instance, Pearson et al. described a whisking pattern with the aim of *'minimal impingement/maximal contact (MIMC)'* [10]. We predict a similar method would be effective for our design, as data from indentations is best below a certain threshold (3 mm), and information at higher contact speeds gives better sensitivity. The benefits of lower levels of indentation mean sensors with a smaller dynamic range but a larger sensitivity could be employed, whilst there is also less risk of damage to the system, if the forces on the whiskers are reduced. Applying this concept, whisker can actively choose its behavior during such a whisking activity given different environments to maximise the information gained, for instance, in modality of texture classification similar to the previous study [8], [12].

Several works, such as those mentioned previously, employ designs of tactile sensor systems with multimodal sensors. These include designs inspired from the human fingertip, [13], [14], contact sensing and active whisker sensors, [10], [12], and designs inspired by insect antennae, [15], [16]. However, most of work in this research field has not specifically addressed the low dimensional information such as the principle components of co-variation in high and low frequency sensory modalities. Although whisking methods have been implemented in several works, little has been done to test find optimal whisking speeds and indentations for movable whiskers.

The design in this paper employs two different sensors, and reflects the fact that in nature, several different transduction techniques, and several different types of nerve endings are used to obtain tactile information about the environment. The method and design in this paper show that biomimicry is a good way to provide new sensors and techniques in robotics.

In conclusion, this paper for the first time provides significant insights into how the whisking behavior is related to the correlation of multiple sensory information presented by the eigeninformation of the covariation of data, which can be used under information gain metrics [17] to identify the texture of an object. As in this paper, only one type of environment was used as the sample, it is interesting to further investigate the eigeninformation of the covariation from multi-modal sensory information under interaction with different types of objects. Together with the information gain metrics, this can lead to a complete texture identification and classification with actively controlled behavior.

ACKNOWLEDGEMENT

This work was supported by the UK Engineering and Physical Sciences Research Council (EPSRC) under grant no: EP/N03211X/1

REFERENCES

[1] A. S. Ahl, "The role of vibrissae in behavior - a status review." *Veterinary Research Communications*, vol. 10, no. 4, pp. 245–268, 1986.

[2] M. Brecht, B. Preilowski, and M. Merzenich, "Functional architecture of the mystacial vibrissae." *Behavioural Brain Research*, vol. 84, no. 1–2, pp. 81–97, 1987.

[3] L. Bosman, A. Houweling, C. B. Owens, N. Tanke *et al.*, "Anatomical pathways involved in generating and sensing rhythmic whisker movements." *Frontiers in Integrative Neuroscience*, vol. 5, 2011.

[4] G. Carvell and D. Simons, "Biometric analyses of vibrissal tactile discrimination in the rat." *Neuroscience*, vol. 10, no. 8, 1990.

[5] L. M. Jones, S. Lee *et al.*, "Precise temporal responses in whisker trigeminal neurons." *J. Neurophysiol*, vol. 92, no. 1, 2004.

[6] R. A. Russell, "Closing the sensor-computer-robot control loop," *Robotics Age*, vol. 6, no. 4, pp. 15–20, 1984.

[7] R. A. Russell and J. A. Wijaya, "Object exploration using whisker sensors," *Australasian Conference on Robotics and Automation*, pp. 180–185, 2002.

[8] M. Fend, "Whisker-based texture discrimination on a mobile robot," *Advances in Artificial Life*, vol. 3630 of the series Lecture Notes in Computer Science, pp. 302–311, 2005.

[9] J. H. Solomon and M. J. Hartmann, "Robotic whiskers used to sense features," *Nature*, vol. 443, no. 7111, p. 525, 2006.

[10] M. Pearson, B. Mitchinson *et al.*, "Biomimetic vibrissal sensing for robots." *Phil. Trans. R. Soc. B*, vol. 366, no. 1581, 2011.

[11] D. Kim and R. Moller, "Biomimetic whiskers for shape recognition," *Robotics and Autonomous Systems*, vol. 55, no. 3, pp. 229–243, 2007.

[12] J. Sullivan, M. Pearson *et al.*, "Tactile discrimination using active whisker sensors," *IEEE Sensors*, vol. 12, no. 2, pp. 350–362, 2012.

[13] D. S. Chathuranga, Z. Wang, Y. Noh, T. Nanayakkara, and S. Hirai, "Robust real time material classification algorithm using soft three axis tactile sensor: Evaluation of the algorithm," in *Intelligent Robots and Systems (IROS), 2015 IEEE/RSJ International Conference on*. IEEE, 2015, pp. 2093–2098.

[14] D. S. Chathuranga, Z. Wang, Y. Noh, , T. Nanayakkara, and S. Hirai, "Disposable soft 3 axis force sensor for biomedical applications," in *Engineering in Medicine and Biology Society (EMBC), 2015 37th Annual International Conference of the IEEE*. IEEE, 2015, pp. 5521–5524.

[15] M. Kaneko, N. Kanayama, and T. Tsuji, "Active antenna for contact sensing," *Robotics and Automation, IEEE Transactions on*, vol. 14, no. 2, pp. 278–291, 1998.

[16] A. G. Lamperski, O. Y. Loh, B. L. Kutscher, and N. J. Cowan, "Dynamical wall following for a wheeled robot using a passive tactile sensor," in *Robotics and Automation, 2005. ICRA 2005. Proceedings of the 2005 IEEE International Conference on*. IEEE, 2005, pp. 3838–3843.

[17] N. Sornkarn, M. Howard, and T. Nanayakkara, "Internal impedance control helps information gain in embodied perception," in *Robotics and Automation (ICRA), 2014 IEEE International Conference on*. IEEE, 2014, pp. 6685–6690.